Consolidation

22

Consolidation with Subpleural or Patchy Distribution

Definition

Consolidation refers to an area of homogeneous increase in lung parenchymal attenuation that obscures the margins of vessels and airway walls [1]. Air bronchograms may be present with consolidative area. Pathologically, consolidation represents an exudate or other product of disease that replaces alveolar air, rendering the lung solid [2, 3].

Diseases Causing the Pattern

Cryptogenic organizing pneumonia (*COP*) (Fig. 22.1), *chronic eosinophilic pneumonia* (*CEP*) (Fig. 22.2), *Churg–Strauss syndrome* (*CSS*) (Fig. 22.3), and *radiation pneumonitis* (Fig. 22.4) usually depict subpleural or patchy areas of consolidation in both lungs.

Distribution

Consolidation in COP is present alone or as part of a mixed pattern and has a predominantly subpleural or peribronchovascular distribution [4]. The consolidation usually involves both lungs and shows middle and lower lung zone predominance [5, 6]. In CEP, CT scans show subpleural consolidation with upper and middle lung zone predominance [7]. Consolidation in CSS is present, usually mixed with other patterns of abnormalities including small nodules and ground-glass opacity (GGO), and shows random distribution [8]. Consolidation in radiation pneumonitis involves uniformly the irradiated lung portion, but not necessarily conforming to the shape of the irradiation portal [9]. The consolidation may show patchy and extensive distribution.

Clinical Considerations

The presence of asthma history suggests the diagnosis of chronic eosinophilic lung disease (almost all patients in CSS and approximately 40 % of patients with CEP) [10]. COP or COP-like lung lesion may be seen in collagen vascular disease, occupational lung disease, or drug-induced lung disease. Abnormal lung lesions like consolidation occur equally in irradiated and unirradiated lung in radiation pneumonitis. This fact, along with prompt improvement of the lesions after corticosteroid therapy, suggests an immunologically mediated mechanism such as a hypersensitivity pneumonitis [11].

Key Points for Differential Diagnosis

	Distribution								Clinical presentations			
	Zones											
Diseases	U	M	L	SP	C	R	BV	R	Acute	Subacute	Chronic	Others
COP		+	+	+			+			+	+	Nodules, reversed halo sign
CEP	+	+		+				+		+	+	Asthma in 40 % of patients
CSS	+	+	+			+		+		+	+	Asthma in all patients, airway disease components
Radiation pneumonitis	+	+	+			+		+		+	+	Usually irradiated region; consolidation beyond irradiated field, hypersensitivity pneumonitis?

Note: *COP* cryptogenic organizing pneumonia, *CEP* chronic eosinophilic pneumonia, *CSS* Churg–Strauss syndrome, *U* upper, *M* middle, *L* lower, *SP* subpleural, *C* central, *R* random, *BV* bronchovascular

K.S. Lee et al., *Radiology Illustrated: Chest Radiology*, Radiology Illustrated,
DOI 10.1007/978-3-642-37096-0_22, © Springer-Verlag Berlin Heidelberg 2014

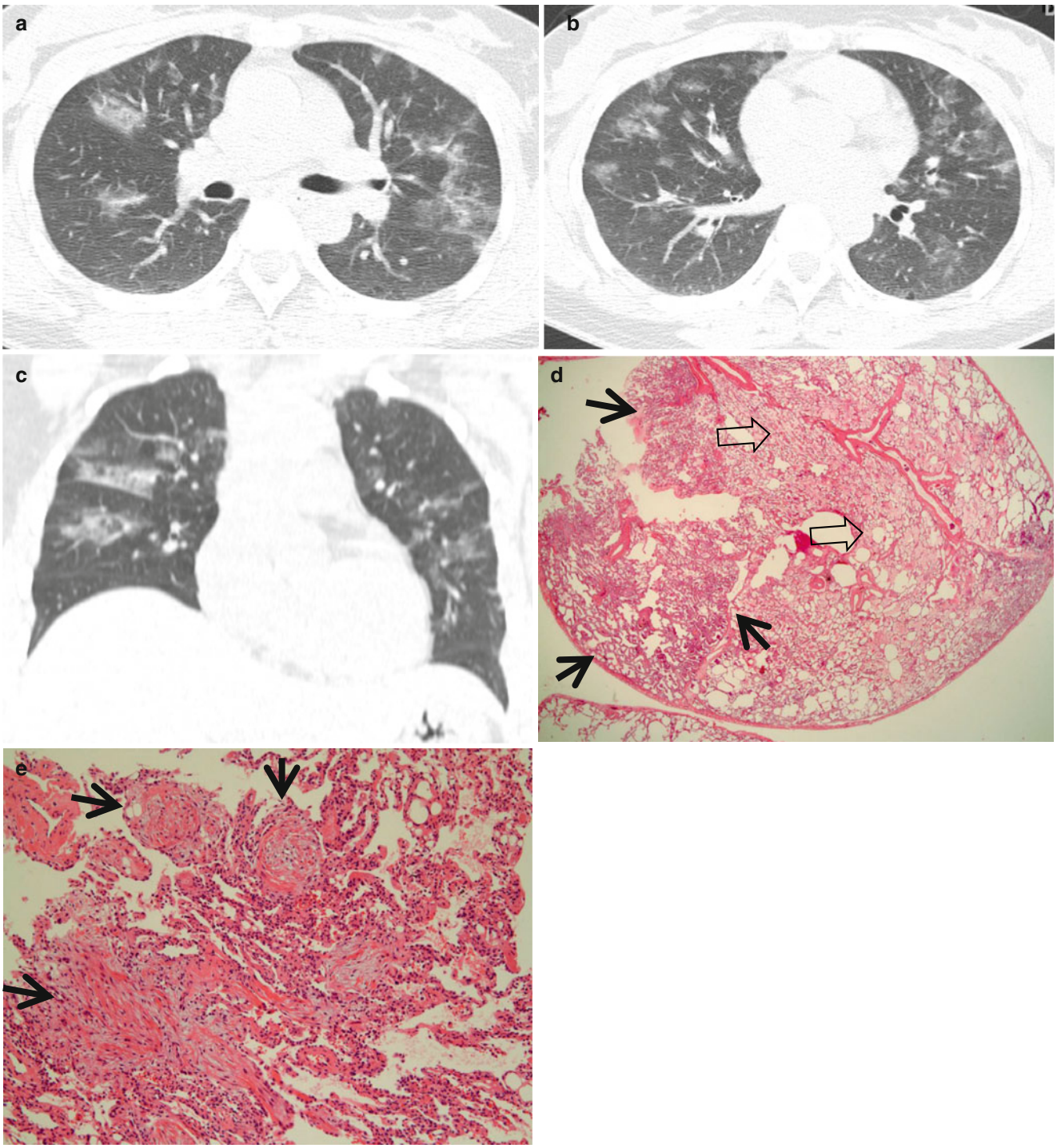

Fig. 22.1 Cryptogenic organizing pneumonia in a 44-year-old woman. (**a**, **b**) Lung window images of CT scans (2.5-mm section thickness) obtained at levels of distal main bronchi (**a**) and inferior pulmonary veins (**b**), respectively, show patchy areas of consolidation, ground-glass opacity, or ground-glass opacity nodules in both lungs. Lung lesions show typically peribronchovascular or subpleural distribution. (**c**) Coronal reformatted image (2.0-mm section thickness) also demonstrates same pattern of lung abnormalities distributed along bronchovascular bundles. (**d**) Low-magnification (×40) photomicrograph of surgical lung biopsy specimen obtained from right middle lobe shows alveolar-filling process with inflammation (*arrows*) and fibrinous exudate (*open arrows*). (**e**) High-magnification (×100) photomicrograph discloses granulation plugs (*arrows*) filling alveolar spaces and alveolar ducts. Patient also has histopathologically some component of capillaritis and alveolar hemorrhage

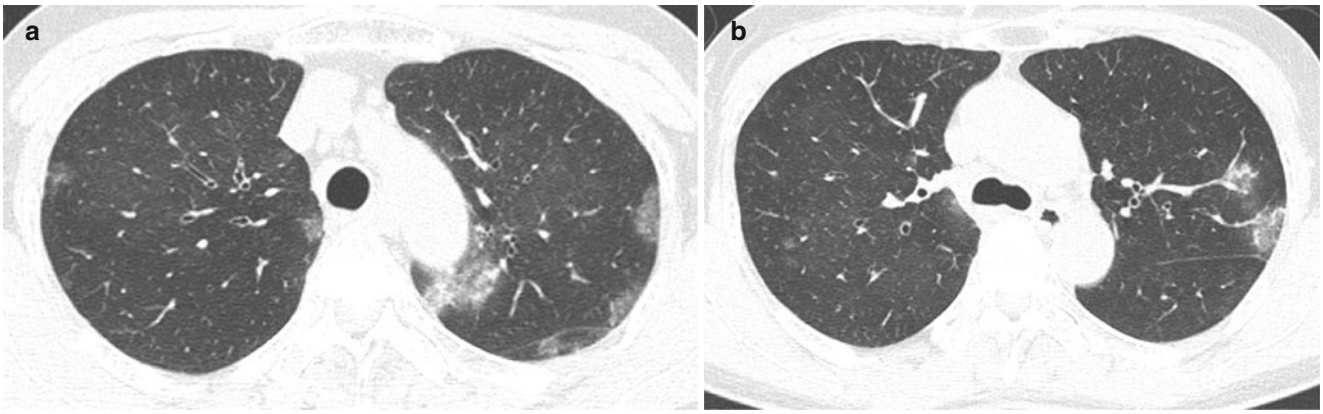

Fig. 22.2 Chronic eosinophilic pneumonia in a 55-year-old asthmatic woman. (**a**, **b**) Lung window images of CT scans (1.5-mm section thickness) obtained at levels of aortic (**a**) and azygos (**b**) arches, respectively, show patchy areas of consolidation and ground-glass opacity in both lungs

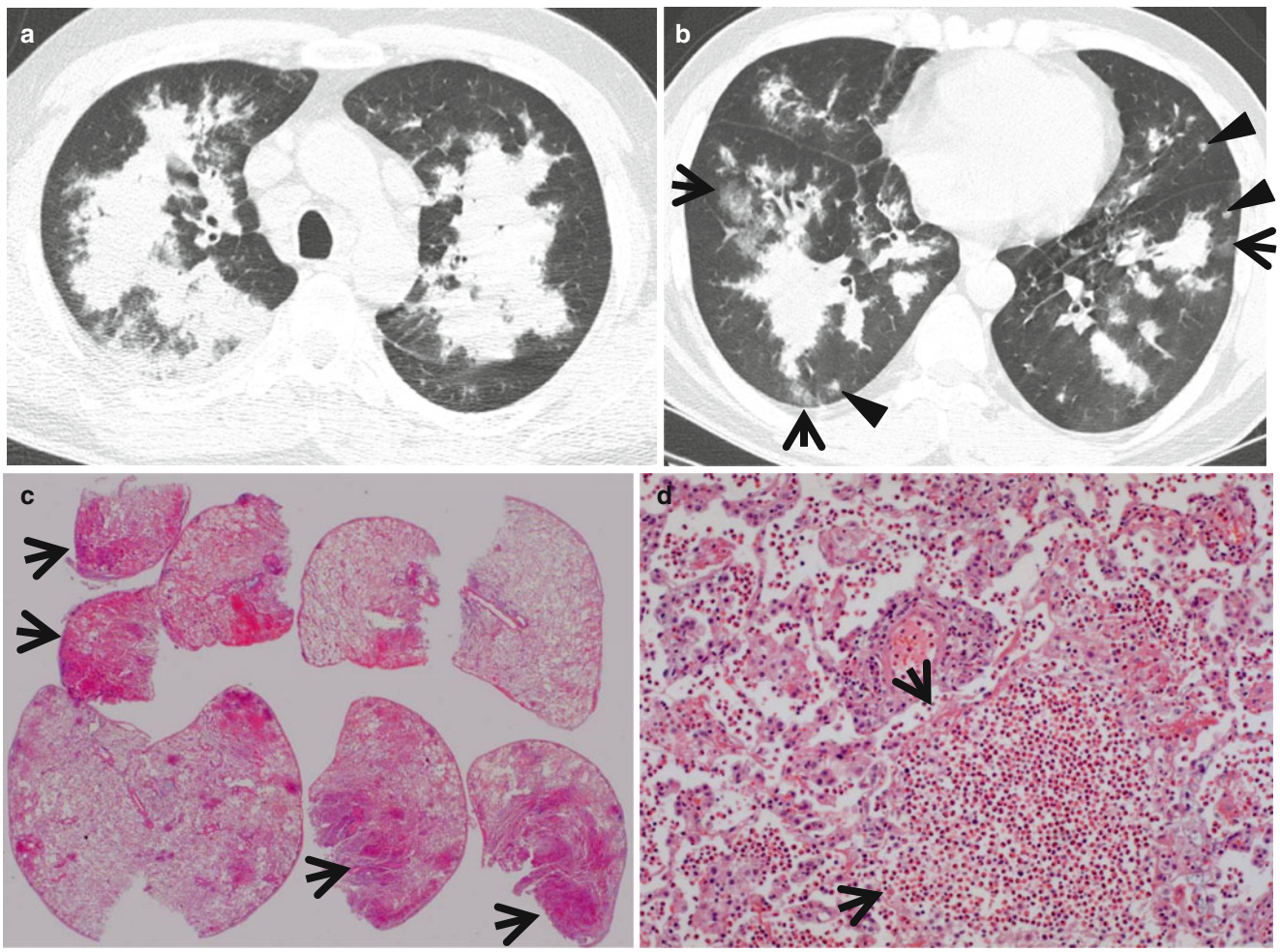

Fig. 22.3 Churg–Strauss syndrome in a 39-year-old asthmatic man. (**a**, **b**) Lung window images of CT scans (2.5-mm section thickness) obtained at levels of aortic arch (**a**) and cardiac ventricle (**b**), respectively, show patchy and extensive areas of consolidation in both lungs. Also note some areas of ground-glass opacity (*arrows*) and poorly defined nodules (*arrowheads*). (**c**) Low-magnification (×40) photomicrograph of surgical lung biopsy specimen obtained from right upper lobe demonstrates alveolar-filling process with eosinophils (*arrows*). (**d**) High-magnification (×100) photomicrograph discloses alveolar spaces filled with eosinophils (eosinophilic pneumonia) (*arrows*). In other areas, small extravascular granulomas and few areas of capillaritis were seen (not shown here)

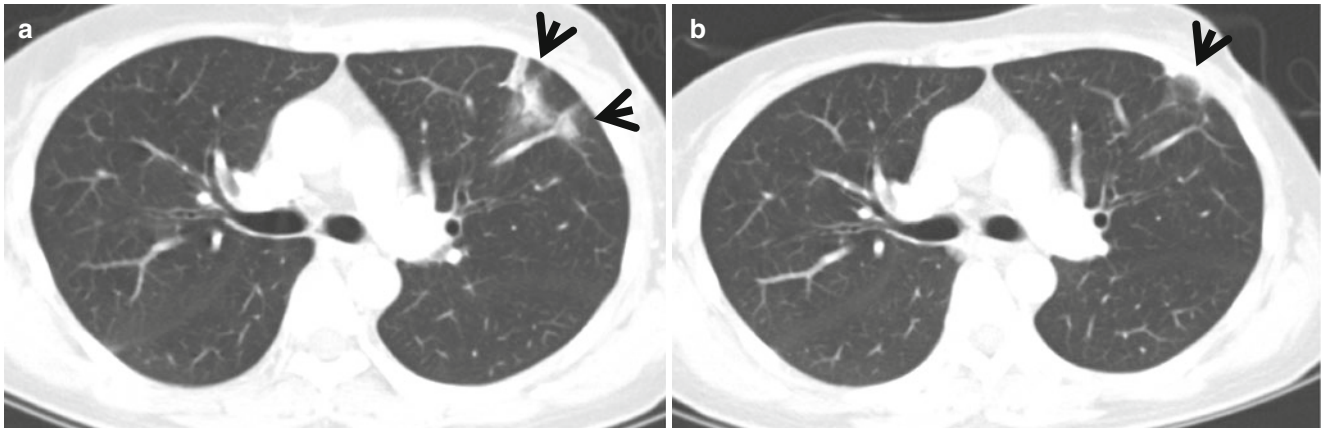

Fig. 22.4 Radiation pneumonitis in a 44-year-old woman with left breast cancer. (**a**, **b**) Lung window images of consecutive CT scans (2.5-mm section thickness) obtained at level of right upper lobar bronchus show focal parenchymal consolidation (*arrows*) in anterior segment of left upper lobe. Patient received conformational irradiation after partial left mastectomy

Cryptogenic Organizing Pneumonia

Pathology and Pathogenesis

COP is characterized by variably dense airspace aggregates of fibroblasts in immature collagen matrix. This alveolar-filling process can be seen to extend into or from terminal bronchioles. Typically, the lung architecture is preserved in COP, and lymphocytes, plasma cells, and histiocytes are present in variable numbers within the interstitium (Fig. 22.1). Fibrin may be seen focally in association with airspace organization. Alveolar macrophage accumulation may be present, attesting to some degree of airway obstruction. Interstitial fibrosis and honeycomb lung remodeling are not components of the cryptogenic (idiopathic) form of organizing pneumonia [12].

Symptoms and Signs

The initial manifestations are nonspecific, with a flu-like illness of fever, malaise, and cough [13]. It is followed by progressive and usually mild dyspnea. Dyspnea may occasionally be severe. In most cases, the duration of onset is less than 3 months. The disease is frequently misdiagnosed as infectious pneumonia. Hemoptysis, chest pain, and night sweating are rare. Finger clubbing is absent. Bibasilar inspiratory crackles are observed at auscultation.

CT Findings

The characteristic HRCT finding of COP consists of unilateral or bilateral areas of airspace consolidation with subpleural or peribronchial distribution [4, 14] (Fig. 22.1). An air bronchogram with bronchial dilatation may be seen in patients who have extensive consolidation, and air bronchograms are usually restricted to these consolidative areas. GGOs are commonly present in association with the areas of consolidation. Curvilinear opacity with an arcade-like appearance (perilobular pattern) is seen in more than half of the patients [15]. Small, ill-defined nodules, often in a centrilobular distribution, are seen in 30–50 % of cases. Occasionally, the disease is manifested as a large nodule or mass-like area of consolidation. Sometimes, COP shows a reversed halo sign, which is defined as central GGO surrounded by more dense airspace consolidation with crescent and ring shapes [5].

CT–Pathology Comparisons

The areas of consolidation correspond histologically to the regions of lung parenchyma that show organizing pneumonia: granulation plugs lying within small airways, alveolar ducts, and alveoli [16] (Fig. 22.1). The GGO correlates with areas of alveolar septal inflammation and minimal airspace fibrosis. The small nodules are related to foci of organizing pneumonia limited to the peribronchial region or to fibroblastic tissue plugs within the bronchiolar lumen. Perilobular pattern pathologically reflects the area of organizing exudate accumulation in the perilobular alveoli, with or without interlobular septal thickening [15]. Reversed halo sign correspond to central area of alveolar septal inflammation and peripheral area of organizing pneumonia within the alveolar ducts [5].

Patient Prognosis

COP responds well to corticosteroids. Corticosteroids result in dramatic clinical improvement, with regression of symptoms within days. The overall prognosis is excellent.

Spontaneous improvement over 3–6 months has been reported. Relapse occurs in 13–58 % of patients on decreasing or after stopping corticosteroid therapy.

Chronic Eosinophilic Pneumonia

Pathology and Pathogenesis

Microscopically, eosinophils fill the alveoli and infiltrate the interstitium (Fig. 22.2). The alveoli also contain a variable number of macrophages. The eosinophil infiltrate may involve small blood vessels but necrotizing vasculitis is not encountered: its presence would suggest Churg–Strauss allergic granulomatosis [17].

Symptoms and Signs

Cough and dyspnea are invariably present [18]. The severity of dyspnea is highly variable from one case to another. Wheezing occurs in about half of the case. Chest pain and hemoptysis are rare. The symptoms are most often present for at least 1 month before diagnosis is made. Weight loss, night sweating, and fever are frequent. The most common extrathoracic manifestations are cardiac, including chest pain with ST segment changes or associated pericarditis.

CT Findings

The characteristic CT finding of CEP is non-segmental areas of airspace consolidation and GGO with peripheral predominance [19, 20] (Fig. 22.2). The consolidation and GGO usually have upper lobe predominance. Less common findings include crazy-paving pattern, nodules, and reticulation. These less common findings predominate in the later stages of CEP. CT performed more than 2 months after the onset of symptoms shows linear band-like areas of parenchymal opacity parallel to the pleural surface. Pleural effusion is observed in less than 10 % of cases.

CT–Pathology Comparisons

Areas of consolidation on HRCT correspond histologically to accumulations of eosinophils and lymphocytes in the alveoli and interstitium and interstitial fibrosis (Fig.22.2).

Patient Prognosis

All the reports have confirmed the dramatic response to corticosteroids. Symptoms and pulmonary infiltrates on imaging improve within a few days of initiation of corticosteroid therapy. However, relapses are observed in up to 50 % of patients while tapering or after stopping the doses of corticosteroids. Long-term corticosteroid therapy is required in more than 50 % of the cases.

Churg–Strauss Syndrome

Pathology and Pathogenesis

The findings on lung biopsy depend on the stage of the disease during which the biopsy is obtained and whether or not the patient has received therapy, particularly steroids. Lung biopsies from CSS patients in the full blown vasculitic phase may show asthmatic bronchitis, eosinophilic pneumonia, extravascular stellate granulomas, and vasculitis (Fig. 22.3). Vasculitis can affect arteries, veins, or capillaries. Diffuse pulmonary hemorrhage and capillaritis can be seen [21].

Symptoms and Signs

Mean age of onset is 38 years. Asthma is essentially universal in CSS [22]. Virtually all patients have eosinophilia. Cardiac involvement is relatively common and is a major cause of mortality. Compared with ANCA-associated granulomatous vasculitis and microscopic polyangiitis, peripheral nerve involvement is more common while pulmonary hemorrhage and glomerulonephritis are much less common.

CT Findings

The most common HRCT findings consist of small centrilobular nodules, GGO, consolidation in a patchy or a predominantly subpleural distribution, bronchial wall thickening and dilatation, interlobular septal thickening, and a mosaic perfusion pattern [8] (Fig. 22.3). Unilateral or bilateral pleural effusion is seen in up to 50 % of patients.

CT–Pathology Comparisons

Small nodules histopathologically correlate with areas of dense eosinophilic and lymphocytic infiltration in the bronchiolar walls and patchy areas of capillaritis in alveolar walls. The areas of consolidation correspond histopathologically to the area of eosinophilic or granulomatous inflammation predominantly in the alveoli and alveolar walls. Interlobular septal thickening may be caused by septal edema, eosinophilic infiltration, and mild fibrosis [8, 23].

Patient Prognosis

Systemic corticosteroids remain the mainstay of therapy. Cyclophosphamide can be used in combination with corticosteroids in cases with severe disease. The mortality rates attributable to CSS or complications of therapy are less than 10–20 %. Older age, azotemia, and cardiac involvement are poor prognostic factors.

Radiation Pneumonitis

Pathology and Pathogenesis

Microscopic findings may include diffuse alveolar damage, acute interstitial pneumonia, and interstitial lymphocytic infiltration in the early phase. There may be variable interstitial, alveolar, and replacement fibrosis in the late phase. Vascular intimal fibrosis with foamy macrophages can be seen [24].

Symptoms and Signs

Symptoms of radiation pneumonitis, including low-grade fever, dry cough, pleuritic chest discomfort, sensation of chest fullness, and dyspnea, usually develop 1–3 months after completion of radiation therapy [25]. In severe cases, patients may present with respiratory failure. Hemoptysis is rare.

CT Findings

The hallmark of radiation pneumonitis on CT is the presence of increased lung attenuation corresponding closely to the location of irradiation ports (Fig. 22.4). Increased lung attenuations include homogeneous GGO that uniformly involves the irradiated portions, patchy consolidation that is contained within the irradiated lung, or discrete consolidation that conforms to the shape of the radiation ports [9, 26]. Subtle GGO or patchy consolidation can be detected outside of the radiation portal in 10–20 % of cases and is less severe than those seen within the radiation ports [9].

CT–Pathology Comparisons

Areas of GGO correspond histologically to airspace and interstitial edema and those of consolidation to diffuse alveolar damage.

Patient Prognosis

Corticosteroids are the mainstay of therapy. It has been shown to improve symptoms and lung function. Signs and symptoms may recur after the cessation of the therapy. Supplemental oxygen may be necessary. Late pulmonary adverse effects include pulmonary fibrosis, which is permanent and associated with marked dyspnea.

Consolidation with Diffuse Distribution

Definition

Consolidation refers to an area of homogeneous increase in lung parenchymal attenuation that obscures the margins of vessels and airway walls [1]. Air bronchograms may be present with consolidative area (Repetition section "Ground-Glass Opacity without Reticulation, Subpleural and Patchy Distribution" in Chap. 21). In certain diseases, the areas of consolidation are widely spread or scattered (diffuse) throughout the lungs.

Diseases Causing the Pattern

Extensive acute pneumonias including viral (Fig. 22.5) and *Pneumocystis* pneumonia, *acute interstitial pneumonia* (*AIP*) (Figs. 22.6 and 22.7) or adult respiratory distress syndrome (ARDS), pulmonary edema, *diffuse alveolar hemorrhage* (*DAH*) (Fig. 22.8) show diffuse areas of consolidation in both lungs.

Distribution

Although diffuse in distribution, subpleural lungs including apices and costophrenic angles may be spared in pulmonary edema and DAH. In *Pneumocystis* pneumonia, the parenchymal lesions may commence in the infrahilar regions and extend to the peripheral lungs. Parenchymal lesions in half of patients with AIP equally involve all three lung zones and those in 39 % of patients have lower lung zone predominance.

Clinical Considerations

Viral pneumonia in adults can be classified into two clinical groups: so-called atypical pneumonia in otherwise healthy hosts and viral pneumonia in immunocompromised hosts.

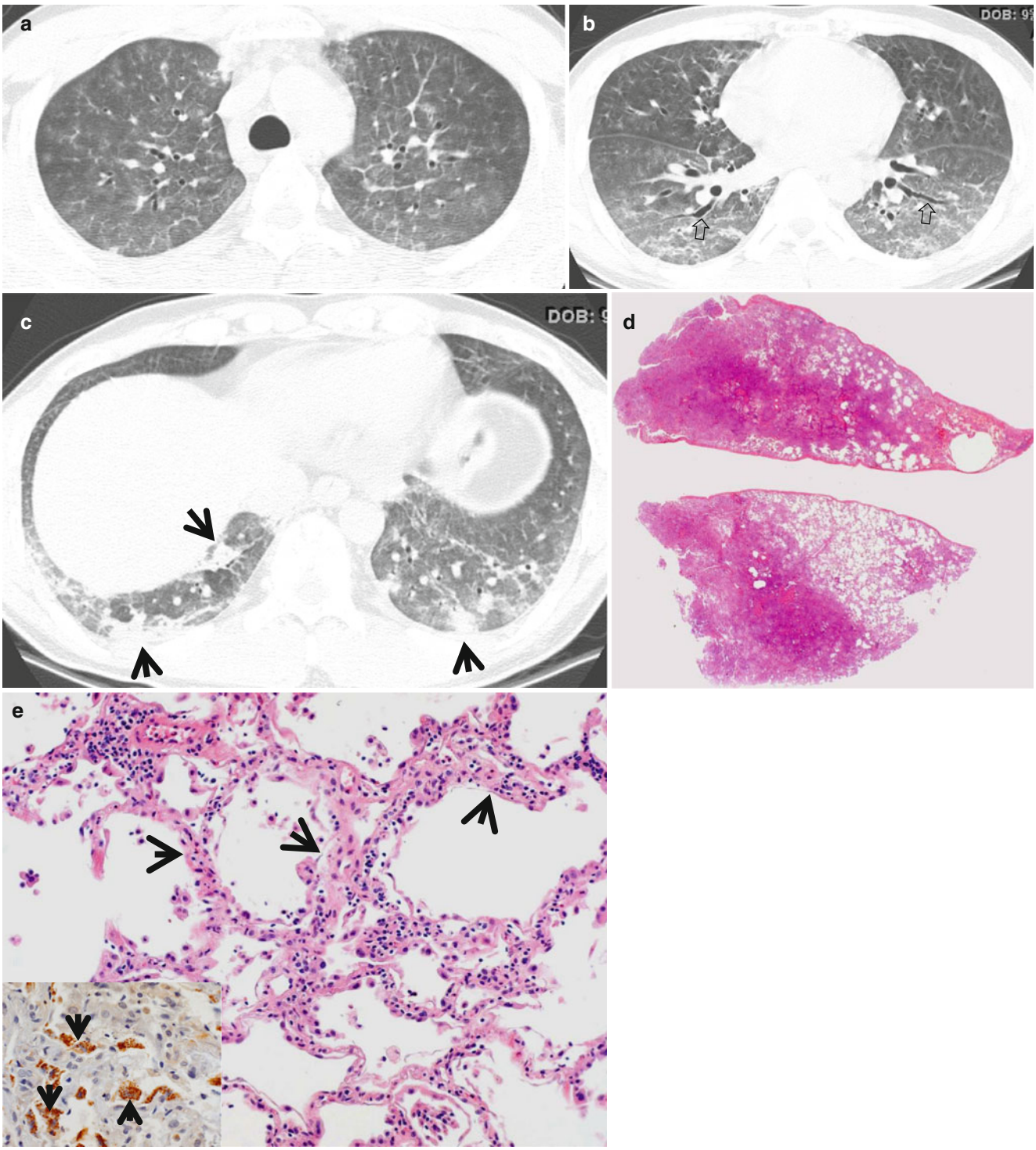

Fig. 22.5 Viral pneumonia presenting as diffuse alveolar damage in a 28-year-old man. Patient has no underlying illness. (a–c) Lung window images of CT scans (2.5-mm section thickness) obtained at levels of azygos arch (**a**), inferior pulmonary veins (**b**), and liver dome (**c**), respectively, show diffuse ground-glass opacity in both lungs and patchy areas of consolidation (*arrows*) in lower lung zones. Also note bronchial dilatation (*open arrows*) in lower lung zones. (**d**) Low-magnification (×10) photomicrograph of surgical biopsy specimen obtained from right upper lobe demonstrates alveolar filling with fibromyxoid tissue admixed with some inflammatory cells. (**e**) High-magnification (×200) photomicrograph focused on interstitial disease process discloses alveolar wall thickening with mononuclear cell and fibroblastic proliferation (*arrows*). *Inset*: immune staining showing many positive particles (*arrows*) in nucleus of pneumocytes

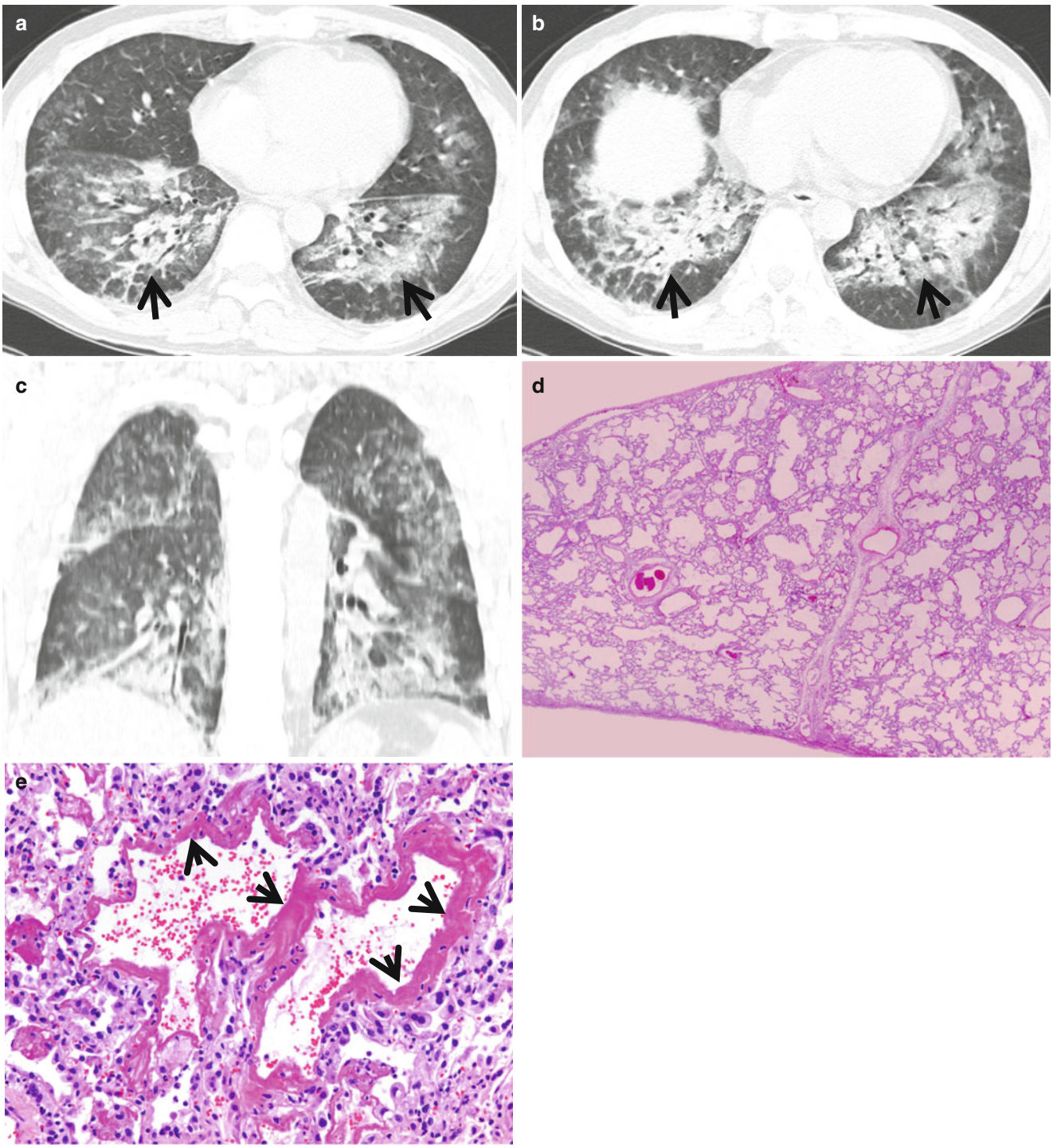

Fig. 22.6 Acute interstitial pneumonia in a 27-year-old man. (**a**, **b**) Lung window images of CT scans (2.5-mm section thickness) obtained at levels of cardiac ventricle (**a**) and liver dome (**b**), respectively, show patchy areas of consolidation and ground-glass opacity in both lungs (*arrows*). (**c**) Coronal reformatted image (2.0-mm section thickness) demonstrates diffuse areas of parenchymal opacity in both lungs. (**d**) Low-magnification (×10) photomicrograph of surgical biopsy specimen obtained from right lower lobe demonstrates diffuse interstitial thickening with edema, fibroblastic proliferation, and mononuclear cell infiltration. (**e**) High-magnification (×200) photomicrograph discloses interstitial fibroblastic proliferation and mononuclear cell (lymphocyte) infiltration. Also note hyaline membranes (*arrows*) lining alveolar walls

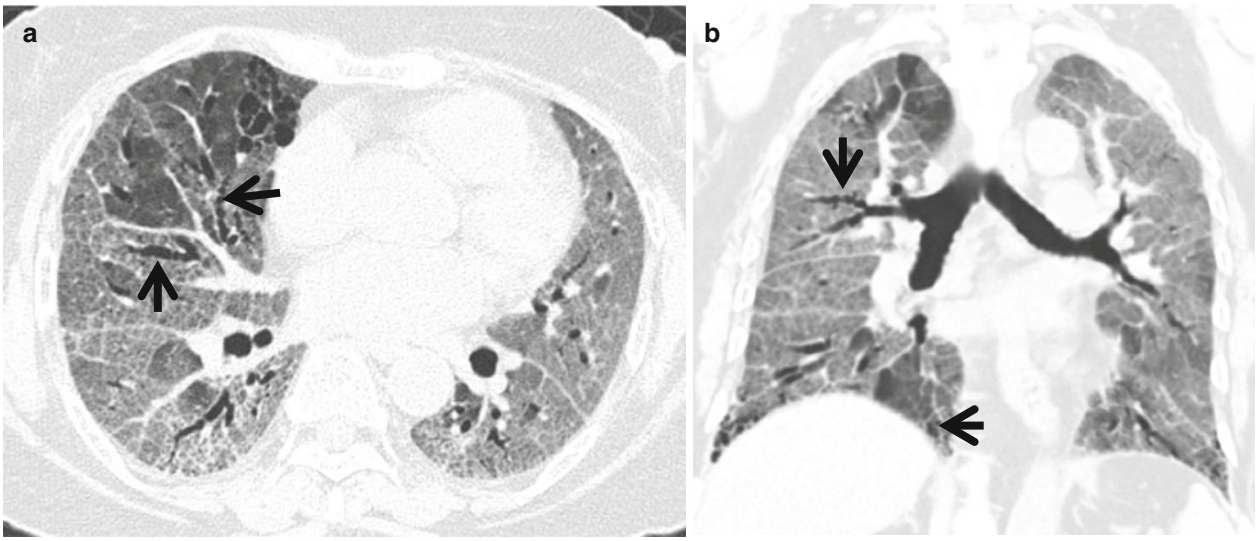

Fig. 22.7 Acute interstitial pneumonia in proliferative phase in a 69-year-old woman. (**a**) Lung window image of CT scans (2.5-mm section thickness) obtained at level of basal trunks shows extensive areas of ground-glass opacity with crazy-paving appearance. Also note traction bronchiectasis (*arrows*) within ground-glass opacity lesions. (**b**) Coronal reformatted image (2.0-mm section thickness) demonstrates diffuse areas of ground-glass opacity and crazy-paving lesions. Also note traction bronchiectasis (*arrows*)

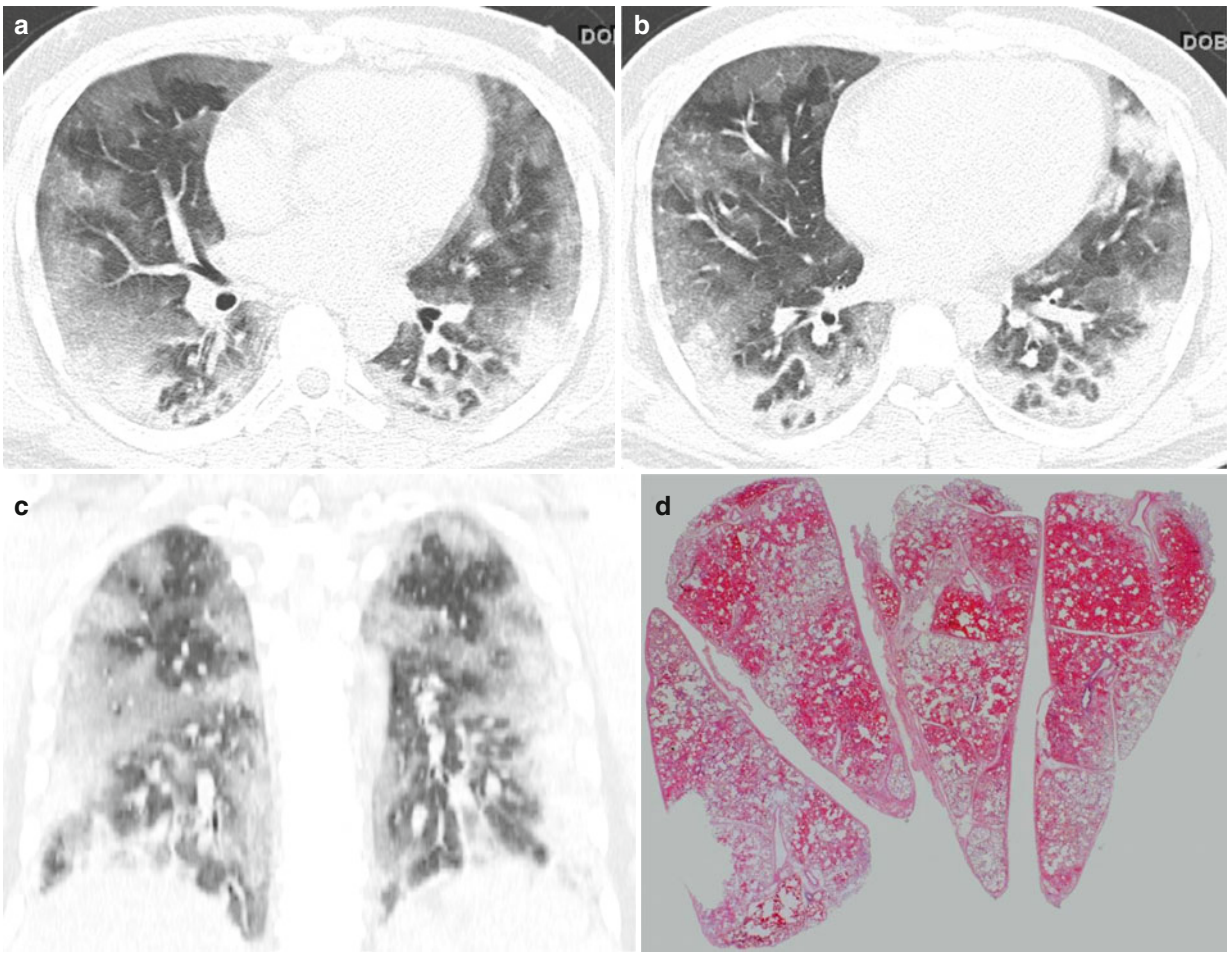

Fig. 22.8 Diffuse alveolar hemorrhage in a 27-year-old man without specific underlying disease identified. (**a**, **b**) Lung window images of CT scans (2.5-mm section thickness) obtained at levels of right middle lobar bronchus (**a**) and segmental bronchi (**b**), respectively, show diffuse areas of parenchymal opacity (consolidation and ground-glass opacity) in both lungs. (**c**) Coronal reformatted image (2.0-mm section thickness) demonstrates diffuse areas of parenchymal opacity in both lungs. (**d**) Low-magnification (×10) photomicrograph of surgical biopsy specimen obtained from right lower lobe exhibits alveolar filling with diffuse intra-alveolar hemorrhage. Specific cause of diffuse alveolar hemorrhage was not elucidated with additional histopathologic studies

Influenza virus types A and B cause most cases of viral pneumonia in immunocompetent adults. Immunocompromised hosts are susceptible to pneumonias caused by cytomegalovirus, herpes virus, measles virus, and adenovirus [27]. AIP is a fulminant disease of unknown etiology, usually occurring in a previously healthy person and producing histologic findings of diffuse alveolar damage (DAD) [28]. CT assessment is potentially helpful in predicting patient prognosis in AIP regardless of physiologic abnormality; namely in survivors, the extent of ground-glass opacity (GGO) or consolidation associated with traction bronchiolectasis or bronchiectasis was less and architectural distortion was also less frequent [29]. ARDS, also called acute respiratory distress syndrome, is a type of lung failure that may result from any disease that causes large amounts of fluid to collect in the lungs (DAD as in AIP). ARDS is not itself a specific disease, but a syndrome, a group of symptoms and signs that make up one of the most important forms of *respiratory failure*. As mentioned in a previous chapter, the most common underlying histology of DAH is of a small vessel vasculitis known as pulmonary capillaritis, usually seen with seropositive systemic vasculitides, or a connective tissue disorder (bland pulmonary hemorrhage), and DAD due to a number of injuries including, drugs, coagulation disorders and infection [30].

Key Points for Differential Diagnosis

	Distribution								Clinical presentations			
	Zones											
Diseases	U	M	L	SP	C	R	BV	R	Acute	Subacute	Chronic	Others
Extensive pneumonia, especially viral pneumonias	+	+	+			+		+	+			Mixed with small poorly defined nodules and GGO lesions
AIP or ARDS	+	+	+			+		+	+			Subpleural lungs are usually involved; CT air-bronchogram sign
Pulmonary edema	+	+	+			+		+	+			Renal edema; apices and costophrenic angles, spared
DAH	+	+	+			+		+	+			Apices and costophrenic angles, spared

Note: *AIP* acute interstitial pneumonia, *ARDS* adult (acute) respiratory distress syndrome, *DAH* diffuse alveolar hemorrhage, *U* upper, *M* middle, *L* lower, *SP* subpleural, *C* central, *R* random, *BV* bronchovascular, *GGO* ground-glass opacity

Viral Pneumonias

Pathology and Pathogenesis

The microscopic findings in most pulmonary viral infections include the direct effect of the virus as well as the host's inflammatory response. The clinical outcome depends upon the virulence of the organism and the nature of the host response; and, consequent pathology includes DAD (Fig. 22.5), diffuse or patchy bronchiolitis and interstitial pneumonitis, giant cell reactions, or even minimal change. The histopathologic diagnosis of viral infection is impossible without the identification of the characteristic cytopathic effect (CPE). DAD, often with bronchiolitis, is the most typical pattern of viral lung injury. However, DAD also occurs in bacterial, mycobacterial, and fungal pneumonias; therefore, a careful search for specific viral CPE becomes important. For the surgical pathologist, CPE manifests mainly as the viral inclusion present in the nucleus or cytoplasm of an infected cell [31].

Symptoms and Signs

In general, clinical manifestations of viral pneumonia are similar to those of bacterial pneumonia. However, wheezing and rhinorrhea are more common while viral pneumonia is less frequently febrile [32]. Mixed or superimposed infection of bacterial agents is common. Acute severe pneumonia progressing to ARDS in viral pneumonia has been increasingly reported.

CT Findings

On CT, viral pneumonia manifests as poorly defined centrilobular small nodules, GGO with a lobular distribution, and segmental consolidation. Because of the presence of associated cellular bronchiolitis, hyperinflation is commonly seen. With progression, the rapid confluence of consolidation leads to DAD (Fig. 22.5), consisting of homogeneous or patchy unilateral or bilateral airspace consolidation and GGO or poorly defined centrilobular nodules [27].

CT–Pathology Comparisons

CT findings of viral pneumonia reflect the variable extents of DAD (intra-alveolar edema, fibrin, and variable cellular infiltrates with a hyaline membrane), intra-alveolar hemorrhage, and interstitial (intrapulmonary or airway) inflammatory cell infiltration (Fig. 22.5).

Patient Prognosis

While therapy for most of viral pneumonia has not been fully clarified, it is reasonable to assume antiviral agents may work if introduced early enough in the course of infection. Viral pneumonia presenting with ARDS requires mechanical ventilation and shows a mortality of 20–25 %.

Acute Interstitial Pneumonia

Pathology and Pathogenesis

Because AIP is idiopathic, other specific causes of acute lung injury must be excluded before making this diagnosis. Considerations in the differential diagnosis include infection, collagen vascular disease, acute exacerbation of idiopathic pulmonary fibrosis (IPF), drug effect, and other causes of DAD. Most cases of DAD are not AIP, and detailed clinical information, radiologic findings, serologic data, and microbiologic results will often point to or rule out a specific etiologic condition. Use of special stains applied to tissue sections or cytologic preparations also is essential to rule out infectious organisms in this setting. AIP is characterized by the histologic pattern of DAD (Fig. 22.6). AIP cannot be distinguished from DAD on histology alone [33].

Symptoms and Signs

AIP can affect patients of any age and sex. The disease if often preceded by a viral-like or flu-like prodromal illness or upper respiratory tract infection characterized by fatigue and myalgia, followed by acute onset of dyspnea, fever and hypoxemia [34]. The duration of symptoms is usually less than 4–8 weeks. The patients have been previously healthy.

CT Findings

The early HRCT findings of AIP consist of patchy or diffuse bilateral GGO and airspace consolidation with interlobular septal and intralobular interstitial thickening [28, 35] (Fig. 22.6). Half of patients have no zonal predominance and 39 % of patients have lower lung zone predominance. With disease progression of disease, the GGO become diffuse, the areas of consolidation become more extensive, and architectural distortion and traction bronchiectasis become evident (Fig. 22.7). Honeycombing is seen in a small percentage of patients.

CT–Pathology Comparisons

Areas of GGO and consolidation without traction bronchiectasis occur in the exudative or early proliferative phase of AIP, whereas traction bronchiectasis is seen in the late proliferative and fibrotic phases of AIP [36]. Honeycombing correlates with the presence of dense interstitial fibrosis and restructuring of distal airspaces.

Patient Prognosis

There is no proven effective therapy. Virtually all patients require mechanical ventilation and supportive care. Many patients are treated with high-dose corticosteroids. The prognosis is poor. Overall, approximately half of patients die within 2 months. However, variable numbers of survivors have been reported [37].

Diffuse Alveolar Hemorrhage

Pathology and Pathogenesis

The histopathology of DAH is stereotypical (Fig. 22.8), regardless of etiology and a specific diagnosis requires clinical and serologic data. Most causes of DAH are immunologically mediated. Some of these diseases have specific patterns of immunoglobulin deposition that can be visualized in tissue sections by using immunofluorescence staining of a specially prepared portion of the surgical lung biopsy. In practice today, immunofluorescence staining is rarely necessary for diagnosis because serologic studies are widely available and reasonably specific for the subtypes of DAH [38].

Symptoms and Signs

Patients with DAH present with cough, dyspnea, and hemoptysis [30]. In fact, one-third of patients will not have hemoptysis, despite active intra-alveolar bleeding. Fever and other systemic symptoms may be present, depending on the etiology of the diffuse alveolar hemorrhage. Careful attention should be given to the nasal and oropharyngeal examination to exclude clues to a vasculitis.

CT Findings

The most common CT features of DAH are bilateral GGOs and consolidation (Fig. 22.8). The lesions are diffuse in the upper and lower lobes in approximately three-fourths of patients or are localized in the lower part of the lungs in 25 % of patients. Typically, the halo sign may be seen with parenchymal nodules or masses and consolidation on CT scans, representing the hemorrhagic nature of these parenchymal lesions. Smooth interlobular septal thickening becomes superimposed on areas of GGO (a crazy-paving appearance) within 2–3 days. These findings may show improvement in the course of hemorrhage resorption.

Additionally, ill-defined centrilobular nodules may be present, reflecting intra-alveolar accumulation of pulmonary macrophages. Nodules have been reported to be uniform in size (1–3 mm in diameter) and are diffusely distributed with no zonal predominance [39].

CT–Pathology Comparisons

The airspace lesions histopathologically correlate with pulmonary hemorrhage, both with or without capillaritis [40] (Fig. 22.8).

Patient Prognosis

The treatment of DAH depends on the underlying cause of hemorrhage. Corticosteroids are a mainstay of therapy in most cases. Cyclophosmide or azathioprine may be added. Plasmapheresis may be tried in the cases of the immune etiology. Mortality is considerable especially in small vessel vasculitis.

References

1. Leung AN, Miller RR, Muller NL. Parenchymal opacification in chronic infiltrative lung diseases: CT-pathologic correlation. Radiology. 1993;188:209–14.
2. Lee KS, Kim EA. High-resolution CT of alveolar filling disorders. Radiol Clin North Am. 2001;39:1211–30.
3. Hansell DM, Bankier AA, MacMahon H, McLoud TC, Muller NL, Remy J. Fleischner Society: glossary of terms for thoracic imaging. Radiology. 2008;246:697–722.
4. Lee KS, Kullnig P, Hartman TE, Muller NL. Cryptogenic organizing pneumonia: CT findings in 43 patients. AJR Am J Roentgenol. 1994;162:543–6.
5. Kim SJ, Lee KS, Ryu YH, et al. Reversed halo sign on high-resolution CT of cryptogenic organizing pneumonia: diagnostic implications. AJR Am J Roentgenol. 2003;180:1251–4.
6. Lee JW, Lee KS, Lee HY, et al. Cryptogenic organizing pneumonia: serial high-resolution CT findings in 22 patients. AJR Am J Roentgenol. 2010;195:916–22.
7. Mayo JR, Muller NL, Road J, Sisler J, Lillington G. Chronic eosinophilic pneumonia: CT findings in six cases. AJR Am J Roentgenol. 1989;153:727–30.
8. Kim YK, Lee KS, Chung MP, et al. Pulmonary involvement in Churg-Strauss syndrome: an analysis of CT, clinical, and pathologic findings. Eur Radiol. 2007;17:3157–65.
9. Libshitz HI, Shuman LS. Radiation-induced pulmonary change: CT findings. J Comput Assist Tomogr. 1984;8:15–9.
10. Kim Y, Lee KS, Choi DC, Primack SL, Im JG. The spectrum of eosinophilic lung disease: radiologic findings. J Comput Assist Tomogr. 1997;21:920–30.
11. Gibson PG, Bryant DH, Morgan GW, et al. Radiation-induced lung injury: a hypersensitivity pneumonitis? Ann Intern Med. 1988;109:288–91.
12. Colby TV. Pathologic aspects of bronchiolitis obliterans organizing pneumonia. Chest. 1992;102:38S–43.
13. Cottin V, Cordier JF. Cryptogenic organizing pneumonia. Semin Respir Crit Care Med. 2012;33:462–75.
14. Muller NL, Staples CA, Miller RR. Bronchiolitis obliterans organizing pneumonia: CT features in 14 patients. AJR Am J Roentgenol. 1990;154:983–7.
15. Ujita M, Renzoni EA, Veeraraghavan S, Wells AU, Hansell DM. Organizing pneumonia: perilobular pattern at thin-section CT. Radiology. 2004;232:757–61.
16. Nishimura K, Itoh H. High-resolution computed tomographic features of bronchiolitis obliterans organizing pneumonia. Chest. 1992;102:26S–31.
17. Allen JN, Davis WB. Eosinophilic lung diseases. Am J Respir Crit Care Med. 1994;150:1423–38.
18. Marchand E, Cordier JF. Idiopathic chronic eosinophilic pneumonia. Semin Respir Crit Care Med. 2006;27:134–41.
19. Johkoh T, Muller NL, Akira M, et al. Eosinophilic lung diseases: diagnostic accuracy of thin-section CT in 111 patients. Radiology. 2000;216:773–80.
20. Jeong YJ, Kim KI, Seo IJ, et al. Eosinophilic lung diseases: a clinical, radiologic, and pathologic overview. Radiographics. 2007;27:617–37; discussion 637–9.
21. Koss MN, Antonovych T, Hochholzer L. Allergic granulomatosis (Churg-Strauss syndrome): pulmonary and renal morphologic findings. Am J Surg Pathol. 1981;5:21–8.
22. Keogh KA, Specks U. Churg-Strauss syndrome. Semin Respir Crit Care Med. 2006;27:148–57.
23. Silva CI, Muller NL, Fujimoto K, Johkoh T, Ajzen SA, Churg A. Churg-Strauss syndrome: high resolution CT and pathologic findings. J Thorac Imaging. 2005;20:74–80.
24. Fajardo LF, Berthrong M. Radiation injury in surgical pathology. Part I Am J Surg Pathol. 1978;2:159–99.
25. Graves PR, Siddiqui F, Anscher MS, Movsas B. Radiation pulmonary toxicity: from mechanisms to management. Semin Radiat Oncol. 2010;20:201–7.
26. Ikezoe J, Takashima S, Morimoto S, et al. CT appearance of acute radiation-induced injury in the lung. AJR Am J Roentgenol. 1988;150:765–70.
27. Kim EA, Lee KS, Primack SL, et al. Viral pneumonias in adults: radiologic and pathologic findings. Radiographics. 2002;22 (Spec No):S137–49.
28. Johkoh T, Muller NL, Taniguchi H, et al. Acute interstitial pneumonia: thin-section CT findings in 36 patients. Radiology. 1999;211:859–63.
29. Ichikado K, Suga M, Muller NL, et al. Acute interstitial pneumonia: comparison of high-resolution computed tomography findings between survivors and nonsurvivors. Am J Respir Crit Care Med. 2002;165:1551–6.
30. Lara AR, Schwarz MI. Diffuse alveolar hemorrhage. Chest. 2010;137:1164–71.
31. Mizgerd JP. Acute lower respiratory tract infection. N Engl J Med. 2008;358:716–27.
32. Cesario TC. Viruses associated with pneumonia in adults. Clin Infect Dis. 2012;55:107–13.
33. Katzenstein AL, Myers JL, Mazur MT. Acute interstitial pneumonia. A clinicopathologic, ultrastructural, and cell kinetic study. Am J Surg Pathol. 1986;10:256–67.
34. Swigris JJ, Brown KK. Acute interstitial pneumonia and acute exacerbations of idiopathic pulmonary fibrosis. Semin Respir Crit Care Med. 2006;27:659–67.
35. Primack SL, Hartman TE, Ikezoe J, Akira M, Sakatani M, Muller NL. Acute interstitial pneumonia: radiographic and CT findings in nine patients. Radiology. 1993;188:817–20.
36. Ichikado K, Johkoh T, Ikezoe J, et al. Acute interstitial pneumonia: high-resolution CT findings correlated with pathology. AJR Am J Roentgenol. 1997;168:333–8.

37. Suh GY, Kang EH, Chung MP, et al. Early intervention can improve clinical outcome of acute interstitial pneumonia. Chest. 2006;129:753–61.
38. Travis WD, Colby TV, Lombard C, Carpenter HA. A clinicopathologic study of 34 cases of diffuse pulmonary hemorrhage with lung biopsy confirmation. Am J Surg Pathol. 1990;14:1112–25.
39. Chung MP, Yi CA, Lee HY, Han J, Lee KS. Imaging of pulmonary vasculitis. Radiology. 2010;255:322–41.
40. Primack SL, Miller RR, Muller NL. Diffuse pulmonary hemorrhage: clinical, pathologic, and imaging features. AJR Am J Roentgenol. 1995;164:295–300.